

Stable Oxidative Cytosine Modifications Accumulate in Cardiac Mesenchymal Cells From Type2 Diabetes Patients

Rescue by α -Ketoglutarate and TET-TDG Functional Reactivation

Francesco Spallotta,* Chiara Cencioni,* Sandra Atlante, Davide Garella, Mattia Cocco, Mattia Mori, Raffaella Mastrocola, Carsten Kuenne, Stefan Guenther, Simona Nanni, Valerio Azzimato, Sven Zukunft, Angela Kornberger, Duran Sürün, Frank Schnütgen, Harald von Melchner, Antonella Di Stilo, Manuela Aragno, Maarten Braspenning, Wim van Criekinge, Miles J. De Blasio, Rebecca H. Ritchie, Germana Zaccagnini, Fabio Martelli, Antonella Farsetti, Ingrid Fleming, Thomas Braun, Andres Beiras-Fernandez, Bruno Botta, Massimo Collino, Massimo Bertinaria, Andreas M. Zeiher, Carlo Gaetano

Rationale: Human cardiac mesenchymal cells (CMSCs) are a therapeutically relevant primary cell population. Diabetes mellitus compromises CMSC function as consequence of metabolic alterations and incorporation of stable epigenetic changes.

Objective: To investigate the role of α -ketoglutarate (α KG) in the epimetabolic control of DNA demethylation in CMSCs.

Methods and Results: Quantitative global analysis, methylated and hydroxymethylated DNA sequencing, and gene-specific GC methylation detection revealed an accumulation of 5-methylcytosine, 5-hydroxymethylcytosine, and 5-formylcytosine in the genomic DNA of human CMSCs isolated from diabetic donors. Whole heart genomic DNA analysis revealed iterative oxidative cytosine modification accumulation in mice exposed to high-fat diet (HFD), injected with streptozotocin, or both in combination (streptozotocin/HFD). In this context, untargeted and targeted metabolomics indicated an intracellular reduction of α KG synthesis in diabetic CMSCs and in the whole heart of HFD mice. This observation was paralleled by a compromised TDG (thymine DNA glycosylase) and TET1 (ten-eleven translocation protein 1) association and function with TET1 relocating out of the nucleus. Molecular dynamics and mutational analyses showed that α KG binds TDG on Arg275 providing an enzymatic allosteric activation. As a consequence, the enzyme significantly increased its capacity to remove G/T nucleotide mismatches or 5-formylcytosine. Accordingly, an exogenous source of α KG restored the DNA demethylation cycle by promoting TDG function, TET1 nuclear localization, and TET/TDG association. TDG inactivation by CRISPR/Cas9 knockout or TET/TDG siRNA knockdown induced 5-formylcytosine accumulation, thus partially mimicking the diabetic epigenetic landscape in cells of nondiabetic origin. The novel compound (S)-2-[(2,6-dichlorobenzoyl)amino]succinic acid (AA6), identified as an inhibitor of α KG dehydrogenase, increased the α KG level in diabetic CMSCs and in the heart of HFD and streptozotocin mice eliciting, in HFD, DNA demethylation, glucose uptake, and insulin response.

Conclusions: Restoring the epimetabolic control of DNA demethylation cycle promises beneficial effects on cells compromised by environmental metabolic changes. (*Circ Res.* 2018;122:31-46. DOI: 10.1161/CIRCRESAHA.117.311300.)

Key Words: DNA methylation ■ epigenomics ■ fibroblasts ■ heart ■ hyperglycemia ■ metabolism

Original received May 6, 2017; revision received November 10, 2017; accepted November 16, 2017. In October 2017, the average time from submission to first decision for all original research papers submitted to *Circulation Research* was 13 days.

From the Goethe University, Frankfurt am Main, Germany (F. Spallotta, C.C., S.A., S.Z., D.S., F. Schnütgen, H.v.M., A.F., I.F., A.M.Z., C.G.); University of Turin, Torino, Italy (D.G., M. Cocco, R.M., A.D.S., M.A., M. Collino, M. Bertinaria); Istituto Italiano di Tecnologia CLNS@Sapienza Rome, Italy (M.M.); Max Planck Institute for Heart and Lung Research, Bad Nauheim, Germany (C.K., S.G., T.B.); Università Cattolica del Sacro Cuore, Rome, Italy (S.N.); Karolinska Institutet, Huddinge, Sweden (V.A.); University of Mainz, Germany (A.K., A.B.-F.); NXT-Dx, Ghent, Belgium (M. Braspenning); Ghent University, Belgium (W.v.C.); Baker IDI Heart and Diabetes Institute, Melbourne VIC, Australia (M.J.D.B., R.H.R.); IRCCS Policlinico San Donato, Milan, Italy (G.Z., F.M.); National Research Council, Rome, Italy (A.F., C.C.); and Sapienza University, Rome, Italy (B.B.).

*These authors contributed equally to this article.

Current address for C. Gaetano: Laboratorio di Epigenetica, Istituti Clinici Scientifici Maugeri, Pavia, Italy.

The online-only Data Supplement is available with this article at <http://circres.ahajournals.org/lookup/suppl/doi:10.1161/CIRCRESAHA.117.311300/-/DC1>.

Correspondence to Prof Carlo Gaetano, MD, Division of Cardiovascular Epigenetics, Department of Cardiology, Goethe University, Frankfurt am Main 60590, Germany. E-mail gaetano@em.uni-frankfurt.de; or Francesco Spallotta, PhD, Division of Cardiovascular Epigenetics, Department of Cardiology, Goethe University, Frankfurt am Main 60590, Germany. E-mail fspallotta@gmail.com

© 2017 American Heart Association, Inc.

Circulation Research is available at <http://circres.ahajournals.org>

DOI: 10.1161/CIRCRESAHA.117.311300

Novelty and Significance

What Is Known?

- Stable epigenetic DNA modifications are introduced in living cells and organs.
- Cellular metabolism regulates function of several epigenetic enzymes.
- Metabolic syndrome or diabetes mellitus alters the cellular epigenetic landscape.
- Specific epigenetic modifications are associated to the onset of metabolic memory.
- Cardiac cells of stromal origin are of therapeutic relevance.

What New Information Does This Article Contribute?

- Ex vivo cultured cardiac mesenchymal cells (CMSCs) from diabetic donors accumulate iteratively oxidized forms of methylated DNA.
- This epigenetic alteration is associated with a reduced intracellular synthesis of α -ketoglutarate (α KG) in vitro and in vivo.
- α KG regulates not only TETs (ten–eleven translocation proteins) but also TDG (thymine DNA glycosylase) activity promoting DNA demethylation in cardiac cells.
- A newly identified drug, inhibiting α KG dehydrogenase, rescued intracellular α KG levels leading to DNA demethylation in vitro and in vivo.

Primary goal of this study has been the multi-OMIC characterization of therapeutically relevant CMSCs of stromal origin isolated from diabetic and nondiabetic donors and observed in a controlled ex vivo environment. In this condition, an elevated content of methylated and iteratively oxidized cytosines was detected globally and in the CpG islands of some cell cycle and metabolically relevant genes. Surprisingly, similar findings were observed in the heart of mice exposed to high-fat diet, injected with streptozotocin, or both in combination (streptozotocin/high-fat diet). In this context, α KG was found reduced in diabetic CMSCs and in the heart of high-fat diet and in streptozotocin mice leading to the TET1/TDG complex disassembly and to a significant decrease of TDG activity. This condition was rescued by supplementing diabetic CMSCs with a cell-permeable form of α KG and, in vivo, by the intraperitoneal administration of (S)-2-[(2,6-dichlorobenzoyl)amino]succinic acid (AA6), a novel inhibitor of the α KG dehydrogenase. Both treatments increased the content of α KG that, acting as an allosteric activator of TDG, triggered DNA demethylation in diabetic CMSCs and in the mouse heart and other organs. As a consequence, glucose uptake, insulin response, and cellular function significantly improved.

Nonstandard Abbreviations and Acronyms

αKG	α -ketoglutarate
5fC	5-formylcytosine
5hmC	5-hydroxymethylcytosine
5mC	5-methylcytosine
CMSC	cardiac mesenchymal cell
D	diabetic
Drp1	dynamitin-like 1 protein
HFD	high-fat diet
IDH	isocitrate dehydrogenase
Irs	insulin response substrate
MD	molecular dynamics
Mfn1	mitofusin1
mrTDG	murine recombinant TDG protein
ND	nondiabetic
OGDH	α KG dehydrogenase
STZ	streptozotocin
TDG	thymine DNA glycosylase
TET	ten–eleven translocation protein

Human cardiac mesenchymal cells (CMSCs) do not naturally exert contractile functions and do not spontaneously generate cardiomyocytes. Under appropriate conditions, however, they may be genetically redirected to differentiate into cardiomyocytes and contribute in situ to cardiac regeneration.¹ These cells are relatively simple to isolate and expand ex vivo² as a population enriched in cells of mesenchymal origin ($\geq 90\%$ CD29-CD90-CD146 positive).² For this reason and thanks to their secretory properties, CMSCs have been recently considered of therapeutic interest for cardiac repair.^{3,4} However, little is still known about the effect of the cardiac metabolic microenvironment

on the biological properties of cardiac nonmyocyte cell populations.⁵

Meet the First Author, see p 3

Clinical trials for type 1 and 2 diabetes mellitus demonstrated that early glycemic control reduces incidence and progression of diabetic complication.⁶ On the other hand, epidemiological and prospective data revealed that in the cardiovascular system diabetes mellitus stressors may persist in spite of glycemic control.⁷ Indeed, a prolonged impairment of glucose homeostasis is a condition that often precedes and accompanies obesity, metabolic syndrome, insulin resistance, and type 1 and 2 diabetes mellitus. The permanent or long-term consequence of an early inefficient glucose handling has been defined as hyperglycemic memory,^{8–10} a phenomenon believed of epigenetic origin¹¹ where specific changes in the histone code and DNA methylation level may provide the mechanistic basis for the perpetuation of an altered metabolic signals.^{12,13} In spite of some advances, how mechanistically epigenetic changes may affect function of CMSCs is still poorly characterized. Recent work, however, provided some evidence that DNA methylation plays an important role in this process.^{14,15}

The recent discovery of α -ketoglutaric acid (α KG)–dependent, iron-dependent, and oxygen-dependent TET (ten–eleven translocation protein)–1,–2,–3 proteins shed light on DNA demethylation mechanisms via conversion of 5-methylcytosine (5mC) into its oxidized forms such as 5-hydroxymethylcytosine (5hmC), 5-formylcytosine (5fC), and 5-carboxylcytosine.¹⁶ The outcome of this process is active demethylation of targeted DNA regions. Remarkably, once acquired, some of the 5mC iterative modifications, including 5hmC and 5fC, remain stable in the DNA of nonregenerating adult mouse organs including brain and heart.^{17,18}

Several epigenetic enzymes contribute to the DNA demethylation process including members of the AID/APOBEC

family and the TDG (thymine DNA glycosylase).^{19,20} In particular, TDG plays a fundamental role, alone or in association with TET1,²¹ in the formation of an abasic site that can be reconverted to unmethylated cytosine with the final contribution of the base excision repair machinery.²² To our knowledge, TDG has never been reported metabolically regulated. The evidence that it may form a complex with TET1,²¹ however, opens up to the possibility that specific pathophysiological metabolic environments, such as those in cancer, chronic inflammation, insulin resistance, or diabetes mellitus, may have implications on TET/TDG function and DNA demethylation.^{23,24}

In the present work, we took advantage from the possibility to isolate human primary CMSCs from diabetic (D-CMSC) and nondiabetic (ND-CMSC) donors analyzing them after few rounds of ex vivo expansion. We found that some important epigenetic alterations resided in D-CMSCs compared with ND-CMSCs cultured in the same condition. Information is reported here about how epigenetic changes were determined in D-CMSCs, with special attention paid to the mechanism of iteratively oxidized DNA cytosine accumulation,²⁵ and how to pharmacologically rescue this alteration.

Methods

All relevant data are available from the authors. The RNA sequencing data sets have been made publicly available at GEO and can be accessed at <https://www.ncbi.nlm.nih.gov/geo/query/acc.cgi?acc=GSE106181>. DNA sequencing data sets are available from the corresponding author on request. All supporting data methods are available as [Online Data Supplement](#).

Results

Accumulation of Methylated Cytosines and Their Iteratively Oxidized Modifications Occurs in Human CMSCs From Diabetic Donors, in the Heart of Mice With Impaired Glucose Homeostasis and in Human Endothelial Cells Exposed to High Glucose

Accumulation of 5mC, and that of its oxidized products, 5hmC and 5fC, occurred in the DNA of human CMSCs obtained from diabetic donors compared with nondiabetic donors (Online Table I; Figure 1A through 1C). Notably, peripheral blood mononuclear cells, isolated from the same diabetic donors did not show a similar pattern for cytosine modifications (Online Figure 1A through 1C). In diabetic peripheral blood mononuclear cells, in fact, only 5fC significantly accumulated (Online Figure 1C), suggesting this modification as one of the oxidized DNA cytosine modifications most sensitive to the

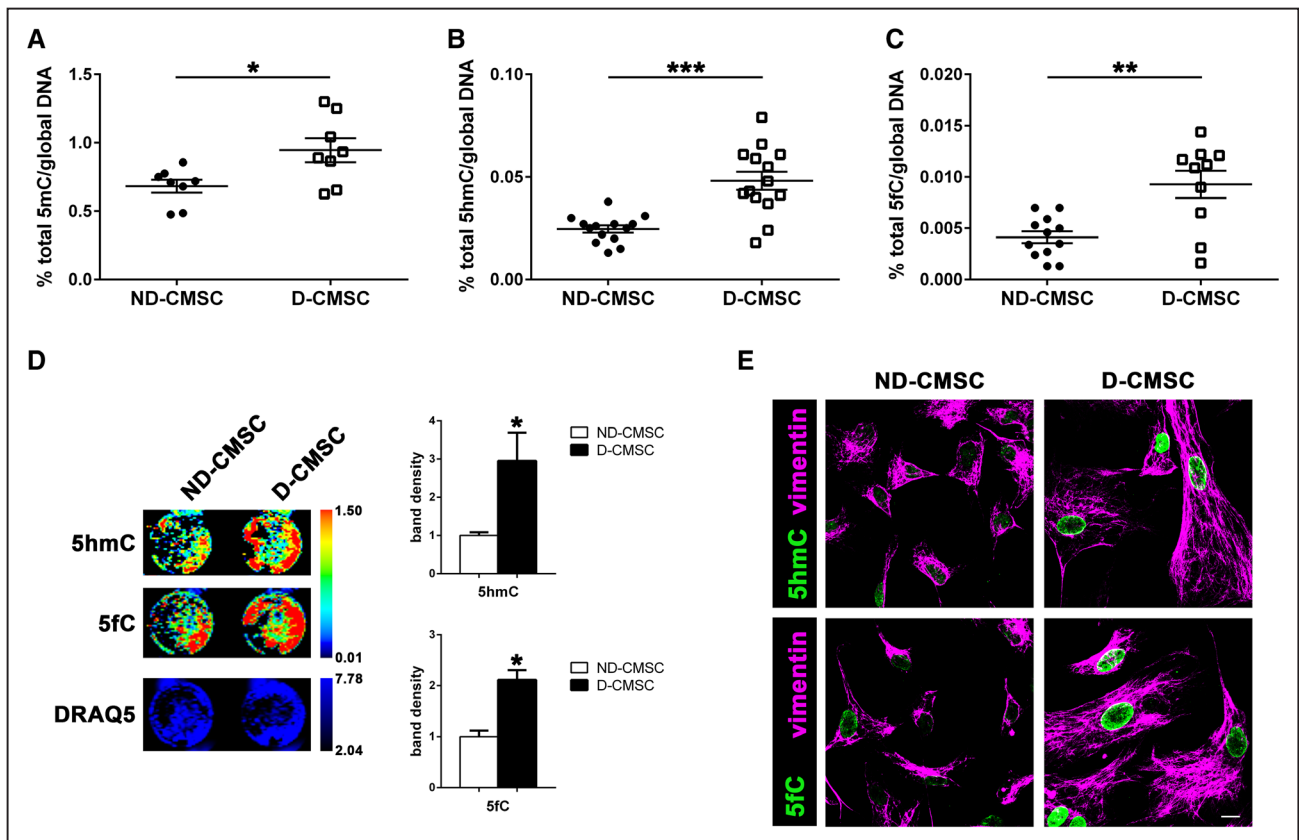


Figure 1. Global 5-cytosine modification increase in human cardiac mesenchymal cells (CMSCs) from diabetic donors. **A**, Quantification of 5-methylcytosine (5mC; n=8), **(B)** 5-hydroxymethylcytosine (5hmC; n=14), and **(C)** 5-formylcytosine (5fC; n=12) in CMSCs isolated from nondiabetic (ND-; black circles) and diabetic (D-; white squares) donors. **D, Left**, Representative in-cell western analysis of ND- and D-CMSCs probed with anti-5hmC and 5fC antibodies. Signals normalized to DNA content according DRAQ5 staining. **Right**, Densitometry of 3 independent experiments. **E**, Representative confocal microscopy images depicting the intracellular content of 5hmC and 5fC in ND- and D-CMSCs. Cells probed by anti-5hmC antibody (green; upper) and anti-5fC antibody (green; lower) and counterstained with vimentin (purple). Scale bar, 10 μ m. Error bars indicate SE. * P <0.05; ** P <0.01; *** P <0.001. Data analyzed by Kolmogorov–Smirnov test.

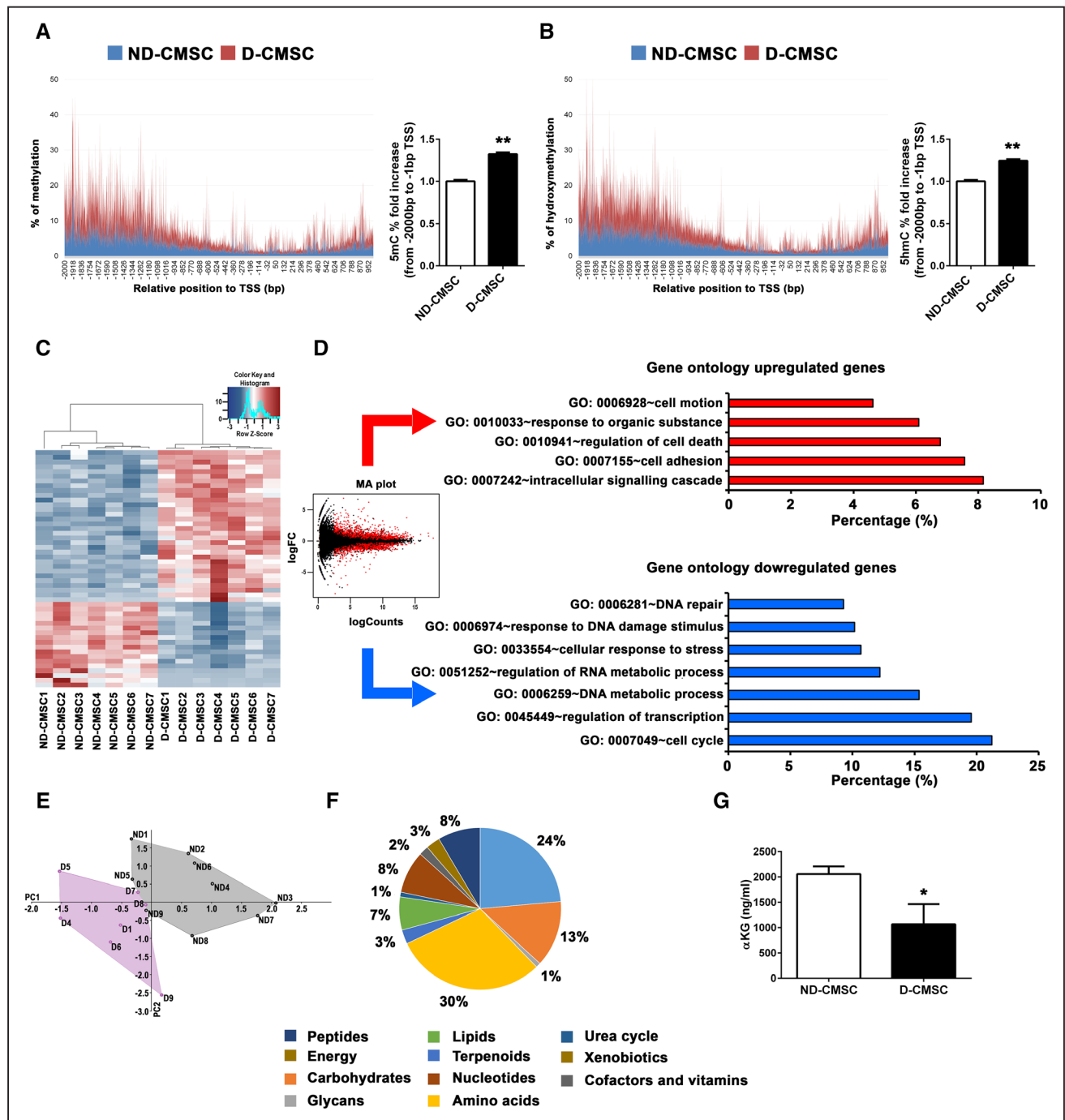


Figure 2. Integrative OMICS approach distinguished human cardiac mesenchymal cells (CMSCs) according to their origin. **A, B, Left,** Cis-regulatory Element Annotation System (CEAS) of 5-methylcytosine (5mC; **A**) and 5-hydroxymethylcytosine (5hmC; **B**) distribution in annotated gene promoter regions of nondiabetic (ND-CMSCs; blue area) and diabetic (D-CMSCs; red area). **x** axis values: -2000 bp to +1000 bp from transcription starting site (TSS). **Right,** Relative 5mC and 5hmC enrichment in the same promoter regions. **C,** Heatmap of 50 most differentially regulated genes in ND- and D-CMSCs by total RNA sequencing. Red and blue colors denote over- and underrepresented genes, respectively. **D, Left,** MA plot of regulated transcripts in ND- and D-CMSCs. Red dots: transcripts with false discovery rate <0.05. **Right,** Gene ontology (GO) analysis. **Upper,** Red bar graph: overrepresented gene families; **(lower)** blue bar graph: underrepresented genes. **E,** Principal component analysis of absolute metabolite levels. Gray-colored convex hull: ND donors; pink-colored convex hull: D donors. Axes are eigenvalue scaled. **F,** Pie chart illustrating GO analysis of annotated and down-modulated metabolites ($P<0.05$) obtained by iPath2 software. **G,** Targeted metabolomic analysis of α -ketoglutarate (α KG) intracellular level in ND- (white bar, $n=4$) and D-CMSCs (black bar, $n=4$). Error bars indicate SE. * $P<0.05$; ** $P<0.01$. Data analyzed by Kolmogorov-Smirnov test.

metabolic environment. These observations, about the accretion of 5hmC and 5fC in D-CMSCs, were confirmed at single cell level by in-cell Western and confocal analyses (Figure 1D

and 1E). Further, exploring 5mC and 5hmC accumulation in the mitochondrial DNA of a subset of randomly chosen human ND- and D-CMSCs, we found a pronounced accumulation of

5hmC in comparison to 5mC (Online Figure ID, right and left, respectively). Of note, there were no apparent differences between cultured ND- and D-CMSCs on 8-oxoguanine accumulation (not shown).

Remarkably, modifications similar to those present in D-CMSCs were observed in the whole heart and in the brain of different animal models of impaired glucose handling such as in high-fat diet (HFD)-fed mice, mice injected with high-dose streptozotocin (STZ), or treated with low-dose STZ plus HFD²⁶ (Online Figures IIA through IIF and XIA through XID). Confocal analysis, performed at the latest experimental

time points, confirmed the presence of 5hmC also in cardiomyocytes of HFD, STZ, and STZ+HFD mice (Figure 6K; Online Figure XIA and XIB). Because of their intrinsically stable inability to handle blood glucose (Online Figure IIE), mice made hyperglycemic by STZ injection were analyzed in greater detail. In them, cardiac DNA hypermethylation, characterized by accumulation of 5mC, 5hmC, and 5fC, became detectable as early as 1 month after blood glucose rose >200 mg/dL. Interestingly, the level of those cytosine modifications remained relatively stable during a time course from 5 to 25 weeks (Online Figure IIG). Accordingly, we found that

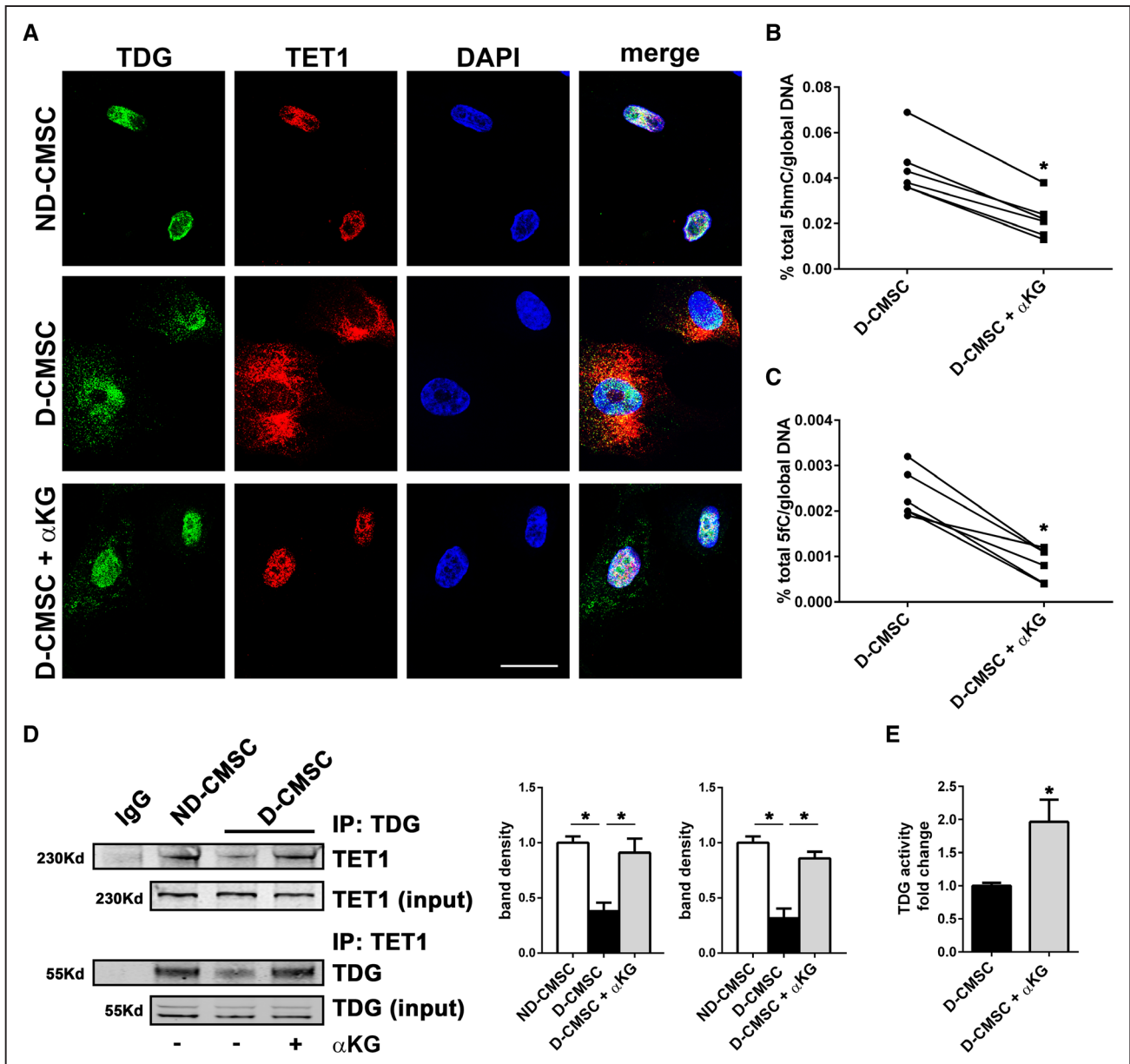


Figure 3. α-ketoglutarate (αKG) triggers TET1 (ten-eleven translocation protein 1)/TDG (thymine DNA glycosylase) association, DNA demethylation, and TDG activation. **A**, Representative confocal microscopy images depicting nondiabetic CMSCs (ND-CMSCs) and diabetic CMSCs (D-CMSCs)±αKG. Cells probed by anti-TDG antibody (green; **left**) and anti-TET1 (red; **middle left**). Nuclei counterstained by DAPI (blue; **middle right**). **Right**, Merged images. **B**, **C**, Quantification of 5-hydroxymethylcytosine (5hmC; **B**) and 5-formylcytosine (5fC; **C**) global levels in D-CMSCs±αKG. **D**, **Left**, Representative co-IP/WB analysis of TET1/TDG complex in ND-CMSCs, D-CMSCs±αKG. **Right**, Densitometry of 3 independent experiments (TET1: **left**; TDG: **right**). **E**, TDG activity of D-CMSCs (black bar), D-CMSCs+αKG (grey bar). Error bars indicate SE. n=6 per condition. **P*<0.05. Data analyzed by Wilcoxon matched-pairs test (**B**, **C**) and Kolmogorov-Smirnov test (**D**, **E**).

a monolayer of confluent human endothelial cells (HUVEC), exposed to high glucose (25 mmol/L) for 72 hours, rapidly accumulated methylated cytosines and their iteratively oxidized forms (Online Figure IIIH through IIJ).

An Integrated OMIC Approach Reveals Altered Functional Pathways in Human CMSCs of Diabetic Origin

The reduced representation of bisulfite genomic sequencing validated the presence of a significant accumulation of 5mC and 5hmC in D-CMSCs. Among the genomic features, modified CpG sequences were abundant in the promoter regions (Figure 2A and 2B). In particular, the coincident presence of 5mC and 5hmC, interested repressed genes involved in transcriptional processes, proliferation, metabolism, and regulation of glucose import (Online Table II), as indicated by gene ontology analysis (Online Figure IIIA).

RNA sequencing, performed in phenotypically consistent but independent subsets of ND- and D-CMSCs, revealed a large number of differentially regulated genes that clearly separated the 2 populations (Figure 2C; Online Table III). Interestingly, the transcripts upregulated in D-CMSCs were involved in matrix synthesis, cell adhesion, signaling, motility,

and apoptosis, consistent with cell activation and death programs (Figure 2D, red bars). The downregulated transcripts (Figure 2D, blue bars), instead, belonged to transcriptional regulation, proliferation, and DNA metabolism, indicative of a potentially causal link with the original pathophysiological environment. Similarly, KEGG pathway analysis indicated extracellular matrix synthesis, cell adhesion, apoptosis, and cytoskeletal remodeling as the most represented pathways (Online Figure IIIB, red bars). Cell metabolism, DNA replication, mismatch, and excision repair were, instead, among the most downregulated functions in D-CMSCs (Online Figure IIIB, blue bars). This evidence prompted us to analyze the metabolome of ND- and D-CMSCs in greater detail. Consistent with the genomic and transcriptomic analyses, D- and ND-CMSCs could be well separated according to their origin (Figure 2E). Untargeted metabolomics of D-CMSCs, in fact, indicated a significant underrepresentation of some metabolites (Online Table IV; Online Figure IVA) belonging to the amino acid, energy, carbohydrate, nucleotide, and other minor metabolic pathways (Figure 2F). The reduced intracellular content of glucose, pyruvate, and α KG was validated by ELISA (Online Figure IVB through IVD). However, because of its relevance in the regulation of DNA demethylases, we further confirmed

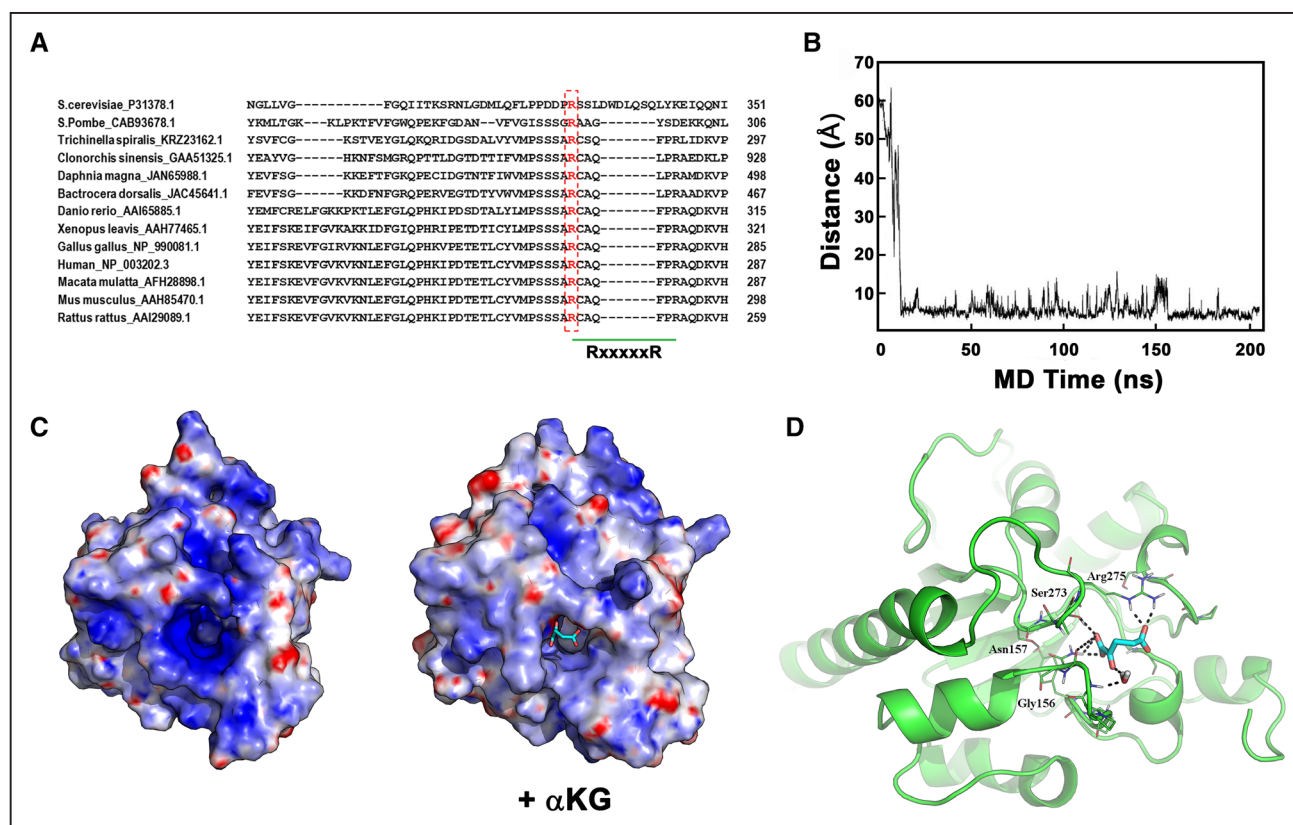


Figure 4. α -ketoglutarate (α KG) acts as an allosteric activator of TDG (thymine DNA glycosylase). **A**, Multiple protein alignment showing arginine (R; red squared) at position 275 in human TDG protein highly interspecies conserved and predicted α KG RxxxxxR binding domain. **B**, α KG binding to TDG investigated by molecular dynamics (MD) simulations. Distance between the centroid of α KG 2 carboxyl groups and of Arginine at position 275 (Arg275) guanidinium group plotted along MD simulation time. **C**, TDG electrostatic surface potential retrieved from x-ray crystallography studies (left) and in complex with α KG as simulated by MD (right). TDG shown as surface. Positively charged regions: blue; negatively charged regions: red; neutral hydrophobic regions: white. Color intensity proportional to charge value. All surfaces calculated at the same salt concentration in aqueous medium. Same orientation of both protein structures. α KG: cyan sticks. **D**, α KG/TDG interaction structural detail in the most populated cluster of conformations taken from MD trajectories. TDG: green cartoon, α KG: cyan sticks. Residues within 6 Å from α KG mass center: lines. H-bond interactions: black dashed lines; TDG residues H-bonded to α KG are labeled.

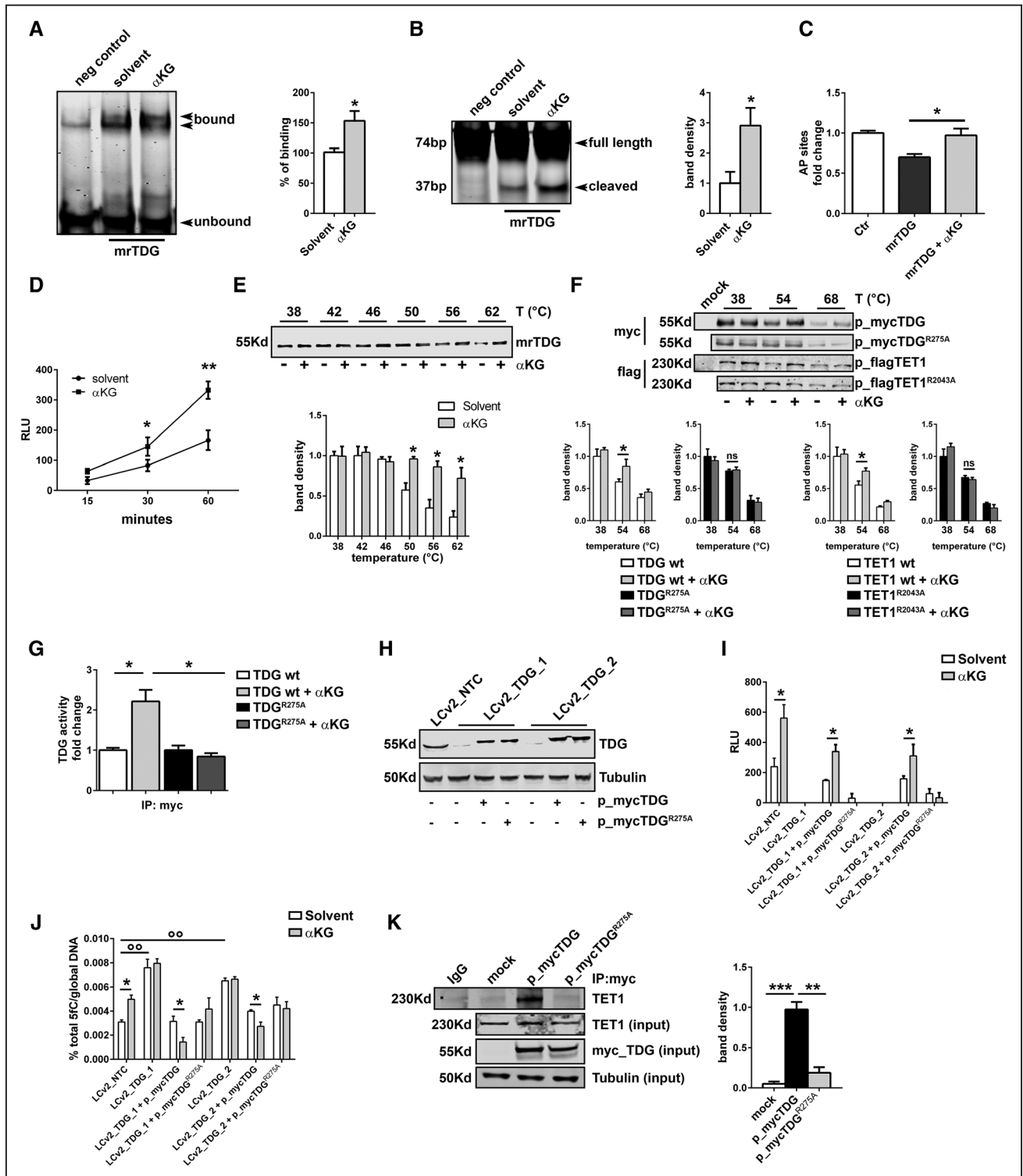


Figure 5. R275 is essential for α -ketoglutarate (α KG) effect on TDG (thymine DNA glycosylase) activity and stability. **A**, Left, EMSA determined by murine recombinant TDG protein (mrTDG)± α KG. The TDG/DNA binding detected by Top_G and Cy5.5_Bot_T primers in equimolar concentration. Signal visualized by Cy5.5 probe. Black arrows: protein-bound and unbound oligo. **Right**, TDG/DNA binding quantification in α KG absence (white bar) or presence (grey bar). Water used as solvent. $n=5$. **B**, Left, G/T glycosylase activity of mrTDG± α KG by Top_G and Cy5.5_Bot_T primers in equimolar concentration. Signal detected by Cy5.5 probe. **Right**, Densitometry of 5 independent experiments of TDG activity in α KG presence (grey bar). Water used as solvent (white bar). **C**, Total abasic site (AP site) number on a reference DNA with mrTDG± α KG. Detection and quantification by aldehyde reactive probe ($n=4$). **D**, TDG activity assay of mrTDG in α KG presence (black squares). Water used as solvent (black circles). **E**, Top, Thermal shift experiments (TSA) performed by mrTDG evaluated at 38°C, 42°C, 46°C, 50°C, 56°C, and 62°C± α KG. Bottom, Densitometry of 5 independent experiments. **F**, Upper, Cell extract thermal shift assay (CETSA)/WB analysis on myc-TDG, myc-TDG^{R275A}, flag-TET1 (ten-eleven translocation protein 1), and flag-TET1^{R2043A} after overexpression in HEK293T cells. Exogenous protein stability tested at 38°C, 54°C, and 68°C± α KG and detected by anti-myc and anti-flag (Continued)

the reduction in α KG intracellular content of D-CMSCs by targeted metabolomics (Figure 2G). In D-CMSCs, a significant reduction of isocitrate dehydrogenase (IDH) activity, the enzyme responsible for α KG synthesis, was detected (Online Figure IVE). A similar finding was observed in HUVEC exposed to high glucose (Online Figure IVF and IVG).²⁷

α KG Rescues Cellular Function in D-CMSCs

Experiments were performed to evaluate the effect of a cell-permeable modified α KG²⁸ administered to D-CMSCs as extracellular source. Notably, α KG rescued cell proliferation (Online Figure VA) and glucose uptake (Online Figure VB). Further genome sequencing revealed a significant enrichment in methylated and hydroxymethylated cytosines in the promoter and coding region of the insulin response substrate 1 and 2 genes (*Irs1* and *Irs2*) in D-CMSCs (Online Figure IIIC). Interestingly, α KG significantly reduced levels of methylation and hydroxymethylation on their promoters (Online Figure VC and VD) in parallel with an increase in the expression at mRNA level (Online Figure VE).

As a potential readout of cellular function, we analyzed the fission/fusion mitochondrial ratio in the presence/absence of α KG. Mitochondrial fission was abundant in isolated D-CMSCs compared with their controls (Online Figure VF through VI). However, in the presence of exogenous α KG, the number of mitochondrial fusion significantly increased (Online Figure VF and VG). This qualitative change was paralleled by a functional recovery as demonstrated by the membrane potential-dependent compound JC-1 green/red color conversion (Online Figure VH and VI). To further investigate this aspect, we evaluated α KG impact on the expression of molecules involved in the mitochondrial fission/fusion conversion and the rate of oxygen consumption. Mfn1 (mitofusin1) was reduced in D-CMSCs; conversely, the Drp1 (dynamin-like 1 protein), abundant during mitochondrial fission, was significantly increased (Online Figure VJ). This phenotype was rescued by α KG treatment. Consistently, rate of oxygen consumption returned to control value in the presence of α KG (Online Figure VK). However, exogenous α KG supplementation was of little or no effect on ND-CMSCs in terms of proliferation (Online Figure VIA), mitochondrial structure (Online Figure VIB and VIC), rate of oxygen consumption (Online Figure VID), and DNA demethylation (Online Figure VIE and VIF).

TET1/TDG Association Is Compromised in Human CMSCs From Type 2 Diabetes Mellitus Patients

To further explore TET/TDG activity in CMSCs, total TET and TDG activities were measured in a series of in vitro assays. Online Figure VIIA and VIIIB show that both enzymes were hypofunctioning in D-CMSCs. This finding was paralleled by the evidence that TET1 and TDG did not associate

well in D-CMSCs (Online Figure VIIC). Intriguingly, experiments with oxalomalic acid, an IDH inhibitor (Online Figure VIID), reproduced the phenotype of D-CMSCs in ND-CMSCs. Specifically, the inhibition of IDH reduced α KG and the TET/TDG association (Online Figure VIIE and VIIF). These results suggest that α KG may be important for TET/TDG complex formation and function. Indeed, they resulted affected in an α KG-reduced intracellular environment like the one of D-CMSCs or of HFD-fed mice heart (see below).

To explore α KG effect, confocal analysis was performed in ND- and D-CMSCs (Figure 3A). As expected, TDG (green) has been found localized to the nucleus. Surprisingly, TET1 (red) localization was nuclear in ND-CMSCs and cytoplasmic in D-CMSCs. This alteration was rescued by adding an α KG extracellular source (Figure 3A). Interestingly, an extranuclear distribution of TET1 was observed in ND-CMSCs treated with okadaic acid, an inhibitor of cellular phosphatases of the PP2a family (Online Figure VIIG). These results were consistent with our prior work, providing evidence that in human endothelial cells, the class II HDAC (histone deacetylases) nuclear localization was sensitive to the action of PP2a (protein phosphatase 2) phosphatase family.²⁹

α KG Triggers TET1/TDG Complex Formation and TDG Activation

Among the multiple roles assigned to α KG, the effect on DNA demethylation was further investigated in our system. Figure 3B and 3C show that the addition of an exogenous source of α KG to D-CMSCs reduced the presence of 5hmC and 5fC in their genomic DNA and that of 5hmC in the mitochondrial one (Online Figure VIIH). This observation suggested that the metabolite triggered an active DNA demethylation process in these metabolically compromised cells.

The experimental evidence that α KG-induced global DNA demethylation including a significant reduction in 5fC prompted us to consider that TDG itself could be sensitive to the intracellular level of this metabolite. No information, however, is currently available on the impact that α KG might have on TET/TDG complex formation²¹ or TDG function per se. Figure 3D shows that TET1/TDG association is significantly improved in D-CMSCs by α KG, an evidence paralleled by the intranuclear relocation of TET1 (Figure 3A, lower). Unexpectedly, Figure 3E shows that an exogenous source of α KG significantly increased TDG activity in cellular extracts obtained from D-CMSCs, thus suggesting for a direct effect of this metabolite on TDG.

α KG Is an Allosteric Cofactor of TDG and Regulates Its Activity

Although no prior knowledge is available about α KG as a potential cofactor/modulator of TDG, we found an α KG-binding consensus motif, RxxxxxR,³⁰ at position 275 to 281

Figure 5 Continued. antibodies. **Lower.** Densitometries of 3 independent experiments. **G,** TDGwt and TDG^{R275A} specific activity in response to α KG. Water used as solvent. Exogenous activity detected after transfection of myc-TDG and myc-TDG^{R275A} in HEK293T cells followed by IP with anti-myc antibody (n=4). **H,** Representative WB of TDG levels in HEK293T cells after CRISPR/Cas9 inactivation (LCv2_TDG_1 and LCv2_TDG_2) compare to control vector (LCv2_NTC). TDG inactivated cells transfected by myc-TDG and myc-TDG^{R275A}. Signal from α -tubulin antibody used as loading control. **I, J,** TDG activity assay (**I**) and 5-formylcytosine (5fC) quantification (**J**) performed in LCv2_NTC, LCv2_TDG_1 and LCv2_TDG_2 \pm myc-TDG and myc-TDG^{R275A} \pm α KG (gray bars). Water used as solvent (white bars). **K, Left,** Representative co-IP/WB analysis of TET1-mycTDG complex formation in HEK293T transfected with myc-TDG or myc-TDG^{R275A}. **Right,** TET1 densitometry of 3 independent experiments. Error bars indicate SE. * P <0.05; ** P <0.01; *** P <0.001; °° P <0.01 vs LCv2_NTC. Data analyzed by Kolmogorov–Smirnov test (**A–C, E–G, I–K**) and 2-way ANOVA (**D**). RLU indicates relative light units.

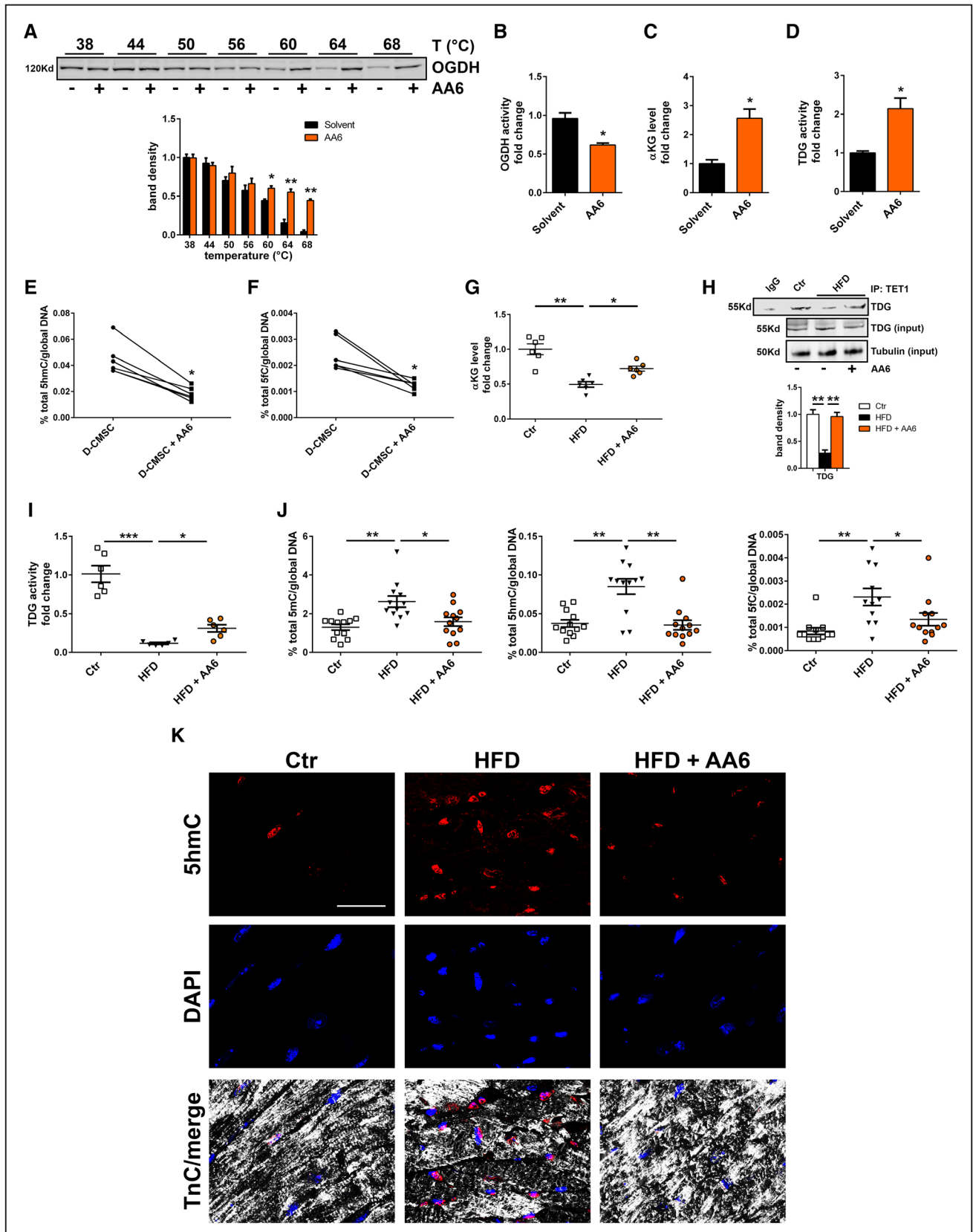


Figure 6. (S)-2-[(2,6-dichlorobenzoyl)amino]succinic acid (AA6) acts along the OGDH- α -ketoglutarate (α KG)/TET (ten-eleven translocation protein)/TDG (thymine DNA glycosylase) pathway. **A**, Upper, α KG dehydrogenase (OGDH) cell extract thermal shift assay (CETSA)/WB analysis in diabetic cardiac mesenchymal cells (D-CMSCs). Protein stability tested at 38°C, 44°C, 50°C, 56°C, 60°C, 64°C, and 68°C \pm AA6. Signals detected by anti-OGDH antibody. **Lower**, Densitometry (n=3). **B**, Intracellular OGDH activity in D-CMSCs treated with AA6 (orange bar). DMSO used as solvent (black bar), n=4. **C**, α KG intracellular level quantification in (Continued)

of the human TDG protein (Figure 4A) similar to that of the RNA demethylase ALKBH5.^{30,31} In this motif, the Arginine at position 275 (Arg275) was the most interspecies conserved residue (Figure 4A). Thus, we speculated that α KG might interact directly with TDG to regulate its function. To explore this possibility, we took advantage from molecular dynamics (MD) simulation. α KG was found to rapidly (≈ 10 ns) approach the TDG protein surface stably binding to the enzyme (Figure 4B). Notably, the metabolite did not access to the catalytic core but remained anchored to the positively charged region at its entrance resulting in a local variation of the electrostatic surface potential (Figure 4C; Online Table VA). A persistent interaction with Arg275 (R275) was established, which was identified as the key determinant for the recognition and interaction between α KG and TDG (Figure 4D). The MD analysis of a TDG R275→Ala (A) mutant (TDG^{R275A}) further substantiated this model by showing a complete loss of affinity between α KG and TDG^{R275A} (Online Figure VIIIA). Moreover, α KG was unable to recognize a preformed TDG/DNA-5fC complex (Online Figure VIIIB). In this context, some H-bond interactions between α KG and TDG resulted in the most populated cluster of MD conformations (37.5% of MD time). Specifically, H-bond interactions were established with Gly156 (also bridged by a water molecule), Asn157, and Ser273 (Online Figure VIIIC). In MD simulation, the binding of α KG to TDG induced a slight conformational change in the loops Pro270-Arg281, Gly149-His158, and Asn191-Gly199, possibly allowing the catalytic active site to accommodate a α KG molecule (Online Figure VIID and VIIIE). Further, to identify the potential relevance of α KG/TDG interaction, additional MD simulations were performed on (1) TDG and DNA bearing 5fC in the TDG catalytic site (DNA-5fC), the structure was adapted from the protein crystallographic data (ID 3UO7)²² and (2) the ternary complex TDG/ α KG/DNA-5fC. These analyses demonstrated that TDG/ α KG preformed complex binds DNA-5fC in a conformationally stable structure (Online Figure VIIF, left; Online Table VA). Specifically, α KG, in the most populated cluster of MD conformations (58.5% of MD time), occupied the TDG catalytic pocket without hampering or competing with the binding to 5fC (Online Figure VIIF, right). Theoretical affinity calculations (Online Table VB) suggest that, in the presence of α KG, TDG has a reduced affinity for its target DNA. Taken together, MD simulations indicated that α KG does not hamper the excision repair mechanism of TDG; rather it might exert an allosteric function with potential consequences for the catalytic activity turnover of the enzyme.

To validate the MD prediction that α KG modulated TDG affinity for its DNA targets, experiments were performed assessing the effect of exogenous α KG on the efficiency of TDG-dependent base excision process and abasic sites binding. Here, evidence is provided that in the presence of α KG, a purified mrTDG (murine recombinant TDG protein) recognized more efficiently a DNA oligo bearing a G/T mismatch (Figure 5A). In parallel, the G/T excision activity of mrTDG was increased about 3-fold by α KG (Figure 5B). Similarly, mrTDG protein recognized genomic DNA abasic site reducing accessibility to the fluorescent aldehyde reactive probe (Figure 5C, black bar). Interestingly, α KG restored aldehyde reactive probe signal to control level (Figure 5C, gray bar) and increased the ability of mrTDG to remove 5fC from a synthetic substrate (Figure 5D). The further evidence that α KG protected the mrTDG protein against degradation in a series of thermal shift experiments³² supported our findings (Figure 5E), about a direct and functionally relevant interaction between α KG and TDG. Conversely, a cell extract thermal shift assay,³³ comparing wild-type and TDG^{R275A} as well as TET1 and the TET1 mutant for the α KG-responsive residue R2043→A (TET1^{R2043A}),³⁴ showed a complete loss of protection by α KG for both mutated proteins (Figure 5F). In this context, the R275A mutation of TDG abrogated α KG effect, supporting the hypothesis that R275 regulates the interaction of TDG with α KG in the context of a metabolite-dependent allosteric activation of the enzyme (Figure 5G). To explore further this evidence, experiments were performed in HEK293T cells in which the endogenous TDG was knocked out by CRISPR/Cas9 technology and reconstituted by transfection of wild-type or mutant TDG. Figure 5H shows a representative Western blotting analysis of 2 independent TDG^{KO} clones and their reconstitution by myc-tagged wild-type or mutant TDG. Figure 5I shows α KG effect treatment on wild-type endogenous TDG before and after reconstitution in the 2 independent CRISPR/Cas9 clones. Always, in the presence of α KG, wild-type TDG activity increased twice above the basal level (Figure 5I, grey columns). The TDG^{R275A} mutant, however, abrogated this effect (Figure 5I). Similarly, TDG abrogation prevented α KG from prompting genomic DNA demethylation, and specifically, the removal of 5fC which accumulated in the absence of TDG or in cells reconstituted with the TDG^{R275A} mutant (Figure 5J). Mechanistically, Figure 5K provides the evidence that TDG^{R275A} variant does not complex with TET1, suggesting that α KG association with TDG may be important for TET/TDG complex formation and demethylation function. Similar results were obtained by siRNA knockdown of TET and TDG in

Figure 6 Continued. D-CMSCs+AA6 (orange bar). DMSO used as solvent (black bar), n=4. **D**, Intracellular TDG activity in D-CMSCs+AA6 (orange bar). DMSO used as solvent (black bar), n=4. **E, F**, Quantification of 5-hydroxymethylcytosine (5hmC; **E**) and 5-formylcytosine (5fC; **F**) global levels in D-CMSCs+AA6. **G**, α KG quantification in the whole heart of Ctr (1.00±0.08), high-fat diet (HFD; 0.49±0.04), and HFD+AA6 (0.72±0.04)-treated mice (n=6). **H, Upper**, Representative co-IP/WB analysis of TET1/TDG complex in Ctr, HFD+AA6-fed mice. **Lower**, Densitometry (Ctr, white bar; HFD: black bar; HFD+AA6: orange bar) n=3. **I**, TDG activity in the whole hearts of Ctr (1.00±0.10), HFD (0.12±0.01) and HFD+AA6 (0.31±0.04) mice (n=6). **J**, Quantification of 5-methylcytosine (5mC; **left**; Ctr 1.30±0.15; HFD 2.62±0.29; HFD+AA6 1.58±0.22), 5hmC (**middle**; Ctr 0.037±0.004; HFD 0.085±0.010; HFD+AA6 0.035±0.006), and 5fC (**right**; Ctr 0.00084±0.00014; HFD 0.00230±0.00037; HFD+AA6 0.00130±0.00027) in whole heart of HFD (black triangles) and HFD+AA6 (orange circles)-fed mice compared with control (white squares; n=12). **K**, Representative confocal microscopy images depicting Ctr, HFD, and HFD+AA6 heart. Cardiac tissue probed by anti-5hmC (red) and anti-Troponin C (TnC, white) antibody. Nuclei counterstained by DAPI (blue). Scale bar, 20 μ m. Error bars indicate SE. * P <0.05; ** P <0.01. *** P <0.001. Data analyzed by Kolmogorov–Smirnov test (**A–D**, **G–J**) and Wilcoxon matched-pairs test (**E**, **F**).

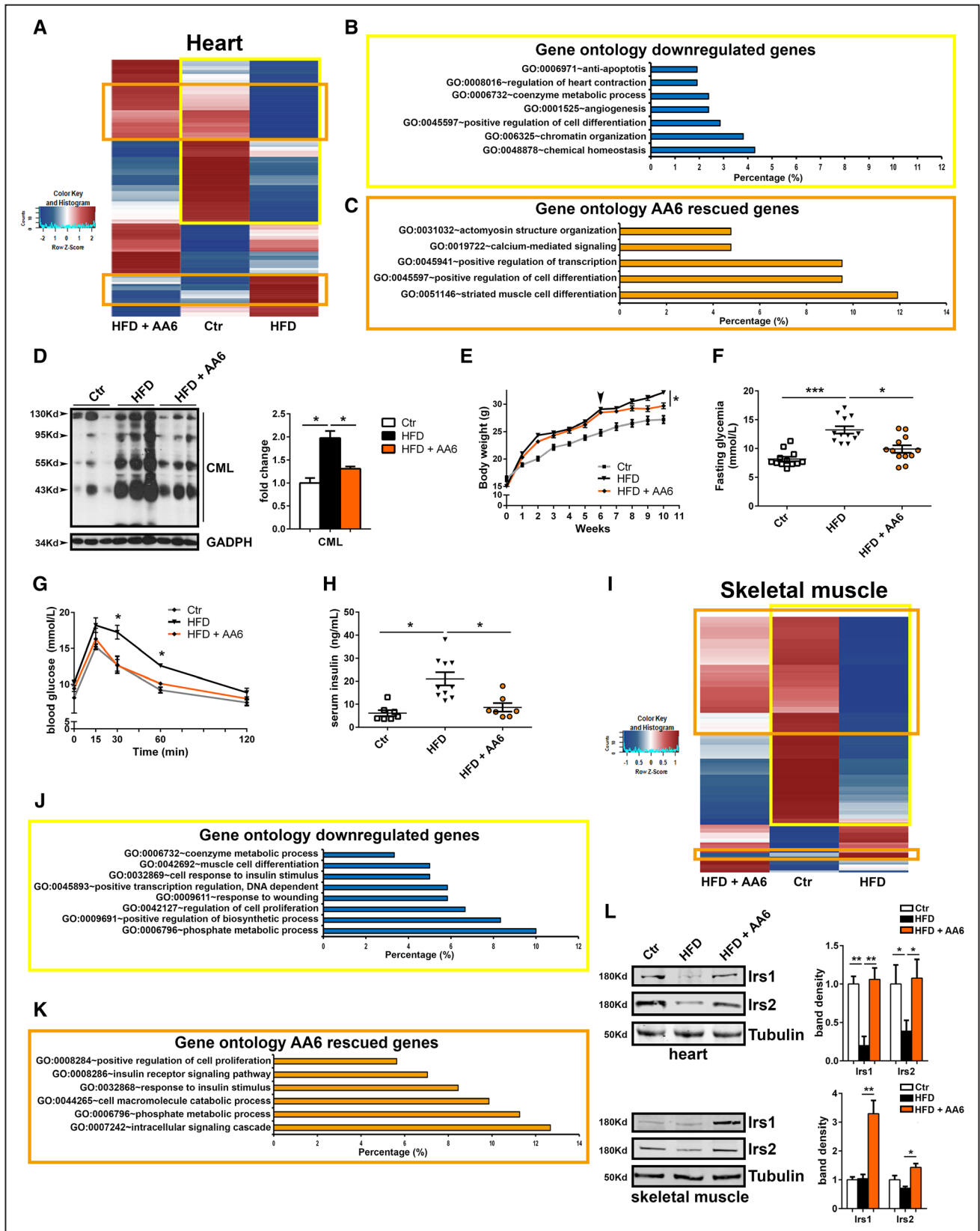


Figure 7. AA6 rescues insulin response in high-fat diet (HFD) mice. **A**, Heatmap showing the 50 most differentially regulated genes in the heart of Ctr, HFD, and HFD+AA6 mice by total RNA sequencing. Red and blue represent over- and underexpressed genes, respectively. Yellow square: genes differentially regulated in HFD animals (n=4). Orange squares: gene expression rescued by HFD+AA6 (n=4). **B**, Gene ontology (GO) analysis of HFD differentially regulated genes in the heart of Ctr and HFD-fed mice (blue bar graph). **C**, GO analysis of AA6-rescued transcripts between HFD-fed mice and those treated with AA6 (orange bar graph). **D**, Left, (Continued)

ND-CMSCs and D-CMSCs. Online Figure IXA through IXE shows that in siRNA, TET/TDG CMSCs 5fC significantly accumulated above control level, and α KG response was abrogated. Further, TDG knockdown in H9C2 cells differentiated into cardiomyocytes^{35,36} (Online Figure IXF) reproduced the deficient phenotype described above indicating that the TDG is active as a DNA demethylation enzymes also in cells of cardiomyogenic lineage (Online Figure IXG and IXH).

A Synthetic α KG Dehydrogenase Inhibitor Rescues Intracellular α KG Levels and Activates TET/TDG Complex Formation and Function Reducing Global DNA Methylation

Hereafter, we investigated whether our findings could be translated into a preclinical setting. Intriguingly, in diabetic patients, α KG plasma concentration has been reported to be similar to that of nondiabetic subjects.³⁷ We extended and confirmed this early observation by using plasma samples collected from donors and from HFD mice (Online Figure XA and XB). In light of this evidence, we reasoned that the intracellular α KG level might be the limiting factor. Considering, in fact, that unmodified α KG is hydrophilic and cannot efficiently cross the plasma membrane,²⁸ it is conceivable that the extracellular part of this metabolite might be ineffective to rescue the alteration in DNA methylation detected in models of impaired glucose homeostasis. To circumvent this problem, we screened a library of small molecules³⁸ for potential regulators of DNA demethylation and identified (S)-2-[(2,6-dichlorobenzoyl)amino]succinic acid (AA6; Online Figure XC) as a direct interactor of α KG dehydrogenase complex (OGDH), determined by cell extract thermal shift assay³³ (Figure 6A). AA6 acts as an enzyme inhibitor (Figure 6B) able to increase α KG intracellular levels (Figure 6C). In the presence of AA6, TDG activity significantly increased (Figure 6D), whereas the global DNA content of 5hmC and 5fC was reduced (Figure 6E and 6F) at an extent similar to that observed after direct administration of the cell-permeable α KG analog (Figure 3B and 3C). Notably, a similar effect was obtained in D-CMSCs by siRNA knockdown of OGDH expression as shown in Online Figure XD through XF. Specifically, the reduction in OGDH expression and function determined an intracellular accumulation of α KG (Online Figure XE) with a small but significant effect on the total DNA content of 5fC (Online Figure XF).

In vivo, in HFD mice fed for 5 weeks and treated daily with AA6 (25 mg/kg) for additional 5 weeks, AA6 increased cardiac α KG levels (Figure 6G), an effect paralleled by the reassembly of TET1/TDG complex (Figure 6H) and TDG

activity gain (Figure 6I). In parallel, 5mC, 5hmC, and 5fC accumulation was normalized (Figure 6J). This observation was further supported by confocal analysis showing positivity for 5hmC in the nuclei of some cardiomyocytes of HFD, STZ, and STZ/HFD mice (Figure 6K; Online Figure XIA and XIB). The number of these nuclei significantly decreased in HFD animals treated with AA6 (Figure 6K). A similar effect was detected in the genomic DNA obtained from the brain of the same animals where 5hmC and 5fC significantly accumulated and diminished after AA6 treatment (Online Figure XIC and XID). Of note, no significant accumulation of modified cytosines was observed in liver with or without AA6, possibly reflecting organ-specific differences in metabolism, pharmacokinetics, or cellular turnover (Online Figure XIC and XID).^{17,18}

Interestingly, during the 5 weeks of AA6 treatment, no adverse reactions to the drug or sudden death episodes occurred. Further, no signs of proliferation or cardiotoxicity were detected (Online Figure XIE and XIF).

AA6 Rescues Glucose Uptake in D-CMSCs and Insulin Response in HFD Mice Promoting Irs1 and Irs2 Expression

During the progress of this work, bioinformatic analysis revealed that in D-CMSCs, compared with ND-CMSCs, Irs1 and Irs2 gene loci were enriched in methylated cytosines at their 5'-region (Online Figure IIIC). In addition, a recent work showed that Irs1 and Irs2 are downregulated in the heart in consequence of an altered metabolic state, a condition typical of HFD mice.³⁹ We reasoned that these 2 genes could be important targets in the glucose response regulation in D-CMSCs and decided to challenge the system with AA6. Remarkably, *Irs1* and *Irs2* loci were methylated and hydroxymethylated in D-CMSCs (Online Figure IIIC). However, AA6 reduced the level of 5mC and 5hmC in the genomic region encompassing *Irs1* and *Irs2* genes (Online Figure XIIA and XIIB) leading to reactivation of gene expression (Online Figure XIIC). This effect was paralleled by an increase of intracellular glucose content in D-CMSCs (Online Figure XIID) and a reassessment of the mitochondrial rate of oxygen consumption at control level, whereas no significant effect was observed in ND-CMSCs (Online Figure XIIE).

Wishing to explore AA6 effect in an in vivo context, a series of experiments were performed in mice exposed to HFD in the presence or absence of the drug. Figure 7A shows the results of RNA sequencing related to the whole heart of

Figure 7 Continued. Representative WB analysis of 3 independent whole heart tissue lysates from Ctr, HFD±AA6 probed with carboxymethyl lysine (CML) antibody. GADPH used as loading control. **Right**, Densitometry. **E**, Animal body weight during standard diet (Ctr) and HFD feeding. Black arrow indicates AA6 starting treatment after 6 wk. Numeric data provided as online. **F**, Blood glucose quantification in Ctr (white squares, n=12; 8.19±0.39), HFD (black triangles, n=12; 13.25±0.63), and HFD+AA6 (orange circles, n=12; 9.91±0.64) mice. **G**, Oral glucose tolerance test (OGTT) in Ctr, HFD, and HFD+AA6 mice. Numeric data provided as online. **H**, Serum insulin level of mice fed with standard diet (Ctr, white squares, n=7; 6.19±1.28), HFD (black triangles, n=10; 21.06±2.82), or HFD+AA6 (orange circles, n=7; 8.67±1.81). **I**, Heatmap showing the 50 most differentially regulated genes in tibialis muscle of Ctr, HFD, and HFD+AA6 by total RNA sequencing. Red and blue represent over- and underexpressed genes, respectively. Yellow square: differentially regulated genes in HFD (n=3). Orange squares: genes rescued by HFD+AA6 (n=3). **J**, GO analysis of HFD differentially regulated genes in tibialis muscle of Ctr and HFD (blue bar graph). **K**, GO analysis of AA6-rescued transcripts in tibialis muscle between HFD-fed mice and HFD+AA6 (orange bar graph). **L**, **Left**, Representative WB analysis of 3 independent tissue extracts from heart (**upper**) and tibialis muscle (**lower**) of Ctr, HFD, and HFD+AA6 mice probed with insulin response substrate 1 and 2 genes (Irs1 and Irs2) antibodies. α -tubulin was used as loading control. **Right**, Densitometry. Error bars indicate SE. * P <0.05; ** P <0.01; *** P <0.001. Data analyzed by Kolmogorov–Smirnov test (**D**, **L**), 1-way ANOVA with Bonferroni post hoc test (**F**, **H**), and 2-way ANOVA (**E**, **G**).

HFD±AA6 mice compared with control condition. Data indicate that HFD significantly changed the pattern of cardiac transcripts which was rescued in HFD animals injected with AA6 (Online Table VI; Figure 7A). In this context, gene ontology analysis revealed that some transcripts associated with important cardiac functions including contractility, metabolism, and homeostasis were compromised (Figure 7B). Notably, treatment with AA6 restored these pathways at control levels with a predominant transcriptional effect on the expression of genes encoding for components of the sarcomeres or proteins involved in calcium handling and cardiac differentiation (Figure 7C). Interestingly, this pattern was at least in part similar to that observed in the transcriptomic analysis of ND- and D-CMSCs (Figure 2D). To explore further the basis of AA6 beneficial effect, we measured the cardiac accumulation of advanced glycation end products, the body weight gain and blood glycemia basal level in HFD mice with or without AA6. In all cases, we observed a positive effect. Specifically, advanced glycation end product accumulation was reduced in HFD animals treated with AA6 (Figure 7D) as well as the body weight gain and the total blood glycemia that showed a significant amelioration in the presence of the drug (Figure 7E and 7F). Further, the effect of AA6 was paralleled by a normalization of the glucose uptake curve (Figure 7G) and the insulin levels (Figure 7H), suggesting for a positive influence on the systemic insulin response. To explore this possibility, RNA sequencing was performed on total RNA extracted from mouse skeletal muscle (Online Table VII; Figure 7I). Similarly to the heart, AA6 treatment had an effect on gene expression with a partial rescue at control level (Figure 7I). Gene ontology analysis indicated that signaling pathways associated with insulin response, metabolism, and differentiation processes were, in fact, depressed in HFD-fed mice (Figure 7J). However, this effect was reverted by AA6 treatment (Figure 7K). Importantly, as seen in D-CMSCs, AA6 promoted *Irs1* and *Irs2* expression in the skeletal muscle and in the heart of HFD+AA6-treated animals (Figure 7L).

Additional experiments, performed in mice made hyperglycemic by STZ and evaluated after 3 months from injection, showed that AA6 failed to restore normal blood glucose (Online Figure XIII A). Nevertheless, the DNA demethylation determined by AA6 treatment occurred in the heart in spite the presence of high blood glucose (Online Figure XIII B through XIII D). This effect was paralleled by an increase of total cardiac α KG level similarly to that seen in HFD mice treated with the drug (Online Figure XIII E; Figure 6G, respectively).

Discussion

Mesenchymal cells are abundant in the cardiac stroma and may either represent a source of regenerating material in the occasion of heart damage and a potential problem in several pathophysiological conditions leading to fibrosis and heart failure.^{5,40,41} In spite of its relevance, little is known about the effect of chronic diseases or metabolic derangements on cardiac stroma and its cellular components. Our prior work reported that CMSCs isolated from patients with clinical history of diabetes mellitus and cultured *ex vivo* demonstrated a variety of epigenetic alterations including the accumulation

of specific histone code modifications and DNA cytosine methylation at cell cycle gene promoters.¹⁴ These observations were compatible with the presence of a hyperglycemic/epigenetic memory phenotype in cells originating from diabetic donors. Recently, we observed that a similar epigenetic landscape was reproduced in the heart of mice after that hyperglycemia was caused by STZ injection (see this work and reference³⁵). This finding reinforced the concept that, in the absence of other pathophysiological conditions, a prolonged period of uncontrolled hyperglycemia^{9,10,15,42,43} could be sufficient to trigger for the introduction of stable and transmissible epigenetic modifications at cellular and organismal level.^{17,18}

Here, we investigated this hypothesis in the attempt to provide mechanistic information about those signals contributing to the accumulation of epigenetic modifications in human CMSCs. Specifically, attention has been paid to those changes having a direct impact on DNA structure and function such as cytosine methylation and its iterative oxidized modifications that have been recently implicated in epigenetic memory transmission.⁴⁴

DNA methylation is emerging as an important epigenetic modification introduced and regulated by a complex network of enzymes whose activity depends on cofactors, such as S-adenosylmethionine or α KG, synthesized during metabolic processes.⁴⁵ Specifically, α KG can regulate DNA and histone methylation level acting on TET1, TET2, TET3 and histone lysine demethylases 2 to 7 (KDM2/7), all members of the so-called 2-oxoglutarate-dependent dioxygenase family.⁴⁶ In particular, TET proteins are responsible of the DNA demethylation process introducing iterative oxidized variants of 5mC like 5hmC, 5fC, and 5-carboxylcytosine that are preparatory for the final removal of the modified cytosine and the reintroduction of the original unmethylated residue.²⁰ Indeed, variation in the α KG availability or synthesis may affect DNA methylation, gene expression, and cellular differentiation.^{47,48}

The recent identification of different iterative cytosine modifications immediately opened the question about their functional role in the regulation of gene expression and their relevance in pathophysiological conditions such as cancer, cardiovascular diseases, or diabetes mellitus.^{49,50} Despite a body of literature indicates that an altered DNA methylation pattern exists in all these situations, the role of the iteratively oxidized cytosine modifications remains unclear.⁵¹ In cancer, the presence of mutations in TET2 gene suggests that its product may be crucial in the process of cellular transformation which may be, at least in part, associated with a deregulated rate of 5mC→5hmC conversion and that of other subsequent modifications.^{52–54} Altogether, the evidence of a deregulation of DNA demethylation through mutations in TET enzymes and in the IDH genes, the enzymes deputed to the synthesis of their cofactor α KG, may provide a new conceptual framework for a better understanding of the interplay among metabolism, DNA methylation, and the onset of specific diseases.⁵⁵ Once acquired, in fact, DNA methylation modifications, such as 5hmC and 5fC, are thought to be stable possibly contributing to epigenetic memory establishment,^{42,45,47,48} a condition still mechanistically poorly understood and largely underestimated at clinical level.

The DNA demethylation process not only requires TET proteins but, to complete the demethylation cycle, other enzymes including TDG must contribute. TDG, in fact, works with TET1 to facilitate 5fC and 5-carboxylcytosine removal from genomic DNA^{21,22} generating abasic sites prone to the reconstitution of unmethylated G:C sequences by members of the AID/APOBEC and base excision repair machinery.⁵⁶ With a similar mechanism, TDG also removes thymine, uracil, and 5-bromouracil from mispairings with guanine and plays a central role in cellular defense against genetic mutation caused by spontaneous deamination of 5mC or cytosine. Of note, when TDG is hypofunctional, a relative genome enrichment in 5fC has been observed.⁵⁷

Although associated to a metabolite-dependent protein such as TET1,²¹ TDG is not known to require metabolites and metals to exert its function. In light of this evidence, the finding described in this article about the TDG association with α KG, which acts as an enzyme allosteric activator, is novel and may contribute to understand how iteratively oxidized cytosines accumulate in cells from the heart of diabetic donors or in organs of animals with impaired glucose handling. In these conditions, TET1/TDG complex is reduced and TDG function compromised. This is a scenario compatible with a defective removal step leading to upstream modified cytosines accumulation. In addition, prediction analysis suggested that in the presence of α KG, the energy of the TDG/DNA/5fC complex increases (Online Table VA). This prediction, the mutation analysis, and the functional evidence of a higher efficiency in mismatched thymine and 5fC removal further support the role of α KG in TDG regulation. Of note, TDG has an intrinsically elevated affinity for the abasic sites that it creates.^{58,59} This association may slow down TDG catalytic turnover requiring post-translational modifications (eg, ubiquitination) and the contribution of other DNA repair enzymes to facilitate TDG release from its target.^{58,59} On the contrary, the allosteric effect of α KG may improve TDG detachment from apyrimidinic sites as suggested by the abasic site measurement. Hence, we speculate here that, although α KG may not be necessary for TDG basal activity, it may be important for its optimal functional turnover.⁶⁰ Our observation may, in fact, represent a case of assisted allosteric activation similar to that reported for the epigenetic enzyme Sirtuin 1 that increases its activity in the presence of synthetic ligands binding the molecule to a single amino acid outside the catalytic site.⁶¹

Noteworthy, during the progress of our work, we identified a new small molecule inhibitor of OGDH, AA6, that acting along the α KG pathway, increased the intracellular α KG, TDG activity, and DNA demethylation in vitro and in vivo. Similarly, OGDH siRNA knockdown largely reproduced the effect of AA6 in CMSCs further supporting the specificity of the new molecule and suggesting a role for OGDH in the control of DNA methylation/demethylation cycle. Indeed, in the presence of AA6, the genomic content of methylated and oxidized cytosines was significantly reduced with evident reactivation signs of the insulin response pathway in D-CMSCs and HFD mice possibly via *Irs1* and *Irs2* reexpression. In parallel, a beneficial effect has been observed on blood glucose and insulin level, body weight gain and glucose response curve.

Although it remains unclear whether this metabolic amelioration has been achieved exclusively through OGDH inhibition and α KG intracellular accumulation or whether AA6 may have additional effects, based on our findings, we may speculate that a dysregulation of IDH/ α KG/OGDH metabolic axis may contribute to the onset of insulin resistance or other metabolic dysfunctions associated to an altered glucose homeostasis. This line of thinking is further reinforced by the evidence that in mice with prolonged hyperglycemia, evaluated after 3 months from STZ injection, AA6 determined cardiac DNA demethylation in the absence of blood glucose normalization. Although more experiments are necessary to fully understand AA6 properties, it is conceivable that it might be the increase in α KG level to determine the beneficial action of this OGDH inhibitor.

Yu et al⁶² reported recently that oxidative stress associated to diabetes mellitus in mice may introduce nitrated residues into OGDH protein with potential consequences on the enzyme function. Our observations, in fact, indicate that the metabolic impairment, associated with the exposure to elevated glucose levels, could lead to variations in the intracellular level of key metabolites, including α KG,⁶³ that in turn could be the *primum movens* underlying the epigenetic DNA modifications possibly associated with an altered glucose homeostasis.^{9,10} α KG response abrogation in the presence of the TDG mutant R275A, TET/TDG complex dissociation determined by the α KG synthesis inhibitor oxalomalic acid, and methylated DNA accumulation seen in the heart of HFD mice and in cellular models, where TET/TDG complex was genetically targeted, are in favor of an important role of α KG contributing to DNA maintenance in our experimental systems.

In conclusion, as depicted in Online Figure XIV, this study suggests that pathophysiological conditions associated with impaired glucose homeostasis, such as diabetes mellitus, may trigger signals in the heart and other organs leading to DNA demethylation machinery alterations as consequence of reduced intracellular α KG content, impaired TDG activity and 5mC, 5hmC, and 5fC accumulation. These alterations are well detectable *ex vivo* in human CMSCs obtained from diabetic donors, and, in our opinion, their damaging effect should be taken into consideration in the context of potential therapeutic applications. In light of this evidence, the new compound AA6 may represent a prototypic metabolic enhancer of DNA demethylation and a new tool to explore the mechanism leading to the incorporation of stable DNA cytosine modifications in cells and tissues. Further experiments are required to elucidate whether α KG level regulation via a calibrated OGDH functional control may represent a new direction for the development of epimetabolic drugs aimed at preventing/reducing consequences of an altered glucose handling. Indeed, the metabolic modulators of DNA demethylation may open novel avenues to the prevention or treatment of the genomic consequences associated with chronic diseases including the functional rescue of therapeutically relevant cardiac cells.⁴

Sources of Funding

The present study was supported by LOEWE Cell & Gene Therapy Center (LOEWE-CGT) Goethe University Frankfurt to C. Gaetano

and by Deutsche Forschungsgemeinschaft Program SFB834 Endothelial Signaling and Vascular Repair, project A9 to I. Fleming, and project B11 to C. Gaetano. F. Spallotta is the recipient of the LOEWE CGT grant no. III L 5-518/17.004 (2013) and funded by the DFG (German Research Foundation), Excellence Cluster Cardio-Pulmonary System. C. Cencioni is the recipient of the Start-up grant 2016 from LOEWE-Forschungszentrum für Zell-und Gentherapie, gefördert durch das Hessische Ministerium für Wissenschaft und Kunst, Aktenzeichen: III L 5-518/17.004 (2013). The present study was supported by Università degli Studi di Torino, Ricerca Locale Quota B 2013 to D. Garella and Quota A 2015 to M. Bertinaria and M. Cocco, by Italian Ministry of Education, University and Research FIRB-MIUR RBFR10URHP_002 and Italian Ministry of Health GR 2011-02351557 to S. Nanni and RF 2010-2318330 to A. Farsetti. This work was supported by Ministero della Salute (Ricerca Corrente, 5X1000, RF-2011-02347907, and PE-2011-02348537), Telethon-Italy (grant no. GGP14092), and AFM Telethon (grant no. 18477) to F. Martelli.

Disclosures

None.

References

- Song K, Nam YJ, Luo X, Qi X, Tan W, Huang GN, Acharya A, Smith CL, Tallquist MD, Neilson EG, Hill JA, Bassel-Duby R, Olson EN. Heart repair by reprogramming non-myocytes with cardiac transcription factors. *Nature*. 2012;485:599–604. doi: 10.1038/nature11139.
- Rossini A, Frati C, Lagrasta C, et al. Human cardiac and bone marrow stromal cells exhibit distinctive properties related to their origin. *Cardiovasc Res*. 2011;89:650–660. doi: 10.1093/cvr/cvq290.
- Guo Y, Wysoczynski M, Nong Y, Tomlin A, Zhu X, Gumpert AM, Nasr M, Muthusamy S, Li H, Book M, Khan A, Hong KU, Li Q, Bolli R. Repeated doses of cardiac mesenchymal cells are therapeutically superior to a single dose in mice with old myocardial infarction. *Basic Res Cardiol*. 2017;112:18. doi: 10.1007/s00395-017-0606-5.
- Wysoczynski M, Guo Y, Moore JB IV, et al. Myocardial reparative properties of cardiac mesenchymal cells isolated on the basis of adherence. *J Am Coll Cardiol*. 2017;69:1824–1838. doi: 10.1016/j.jacc.2017.01.048.
- Cencioni C, Atlante S, Savoia M, Martelli F, Farsetti A, Capogrossi MC, Zeiher AM, Gaetano C, Spallotta F. The double life of cardiac mesenchymal cells: epimetabolic sensors and therapeutic assets for heart regeneration. *Pharmacol Ther*. 2017;171:43–55. doi: 10.1016/j.pharmthera.2016.10.005.
- White NH, Sun W, Cleary PA, Tamborlane WV, Danis RP, Hainsworth DP, Davis MD; DCCT-EDIC Research Group. Effect of prior intensive therapy in type 1 diabetes on 10-year progression of retinopathy in the DCCT/EDIC: comparison of adults and adolescents. *Diabetes*. 2010;59:1244–1253. doi: 10.2337/db09-1216.
- Zhang L, Chen B, Tang L. Metabolic memory: mechanisms and implications for diabetic retinopathy. *Diabetes Res Clin Pract*. 2012;96:286–293. doi: 10.1016/j.diabres.2011.12.006.
- Roy S, Sala R, Cagliero E, Lorenzi M. Overexpression of fibronectin induced by diabetes or high glucose: phenomenon with a memory. *Proc Natl Acad Sci USA*. 1990;87:404–408.
- Cencioni C, Spallotta F, Greco S, Martelli F, Zeiher AM, Gaetano C. Epigenetic mechanisms of hyperglycemic memory. *Int J Biochem Cell Biol*. 2014;51:155–158. doi: 10.1016/j.biocel.2014.04.014.
- El-Osta A. Glycemic memory. *Curr Opin Lipidol*. 2012;23:24–29. doi: 10.1097/MOL.0b013e32834f319d.
- Cooper ME, El-Osta A. Epigenetics: mechanisms and implications for diabetic complications. *Circ Res*. 2010;107:1403–1413. doi: 10.1161/CIRCRESAHA.110.223552.
- Keating ST, Plutzky J, El-Osta A. Epigenetic changes in diabetes and cardiovascular risk. *Circ Res*. 2016;118:1706–1722. doi: 10.1161/CIRCRESAHA.116.306819.
- Rodriguez H, Rafahi H, Bhavne M, El-Osta A. Metabolism and chromatin dynamics in health and disease. *Mol Aspects Med*. 2017;54:1–15. doi: 10.1016/j.mam.2016.09.004.
- Vecellio M, Spallotta F, Nanni S, et al. The histone acetylase activator pentadecylidenemalonate 1b rescues proliferation and differentiation in the human cardiac mesenchymal cells of type 2 diabetic patients. *Diabetes*. 2014;63:2132–2147. doi: 10.2337/db13-0731.
- Keating ST, El-Osta A. Epigenetic changes in diabetes. *Clin Genet*. 2013;84:1–10. doi: 10.1111/cge.12121.
- Ito S, D'Alessio AC, Taranova OV, Hong K, Sowers LC, Zhang Y. Role of Tet proteins in 5mC to 5hmC conversion, ES-cell self-renewal and inner cell mass specification. *Nature*. 2010;466:1129–1133. doi: 10.1038/nature09303.
- Bachman M, Uribe-Lewis S, Yang X, Burgess HE, Iurlaro M, Reik W, Murrell A, Balasubramanian S. 5-Formylcytosine can be a stable DNA modification in mammals. *Nat Chem Biol*. 2015;11:555–557. doi: 10.1038/nchembio.1848.
- Bachman M, Uribe-Lewis S, Yang X, Williams M, Murrell A, Balasubramanian S. 5-Hydroxymethylcytosine is a predominantly stable DNA modification. *Nat Chem*. 2014;6:1049–1055. doi: 10.1038/nchem.2064.
- Scourzac L, Mouly E, Bernard OA. TET proteins and the control of cytosine demethylation in cancer. *Genome Med*. 2015;7:9. doi: 10.1186/s13073-015-0134-6.
- Shen L, Song CX, He C, Zhang Y. Mechanism and function of oxidative reversal of DNA and RNA methylation. *Annu Rev Biochem*. 2014;83:585–614. doi: 10.1146/annurev-biochem-060713-035513.
- Weber AR, Krawczyk C, Robertson AB, Kuśnierczyk A, Vågbo CB, Schuermann D, Klungland A, Schär P. Biochemical reconstitution of TET1-TDG-BER-dependent active DNA demethylation reveals a highly coordinated mechanism. *Nat Commun*. 2016;7:10806. doi: 10.1038/ncomms10806.
- Zhang L, Lu X, Lu J, Liang H, Dai Q, Xu GL, Luo C, Jiang H, He C. Thymine DNA glycosylase specifically recognizes 5-carboxylcytosine-modified DNA. *Nat Chem Biol*. 2012;8:328–330. doi: 10.1038/nchembio.914.
- Chia N, Wang L, Lu X, Senut MC, Brenner C, Ruden DM. Hypothesis: environmental regulation of 5-hydroxymethylcytosine by oxidative stress. *Epigenetics*. 2011;6:853–856.
- Efimova EV, Takahashi S, Shamsi NA, Wu D, Labay E, Ulanovskaya OA, Weichselbaum RR, Kozmin SA, Kron SJ. Linking cancer metabolism to DNA repair and accelerated senescence. *Mol Cancer Res*. 2016;14:173–184. doi: 10.1158/1541-7786.MCR-15-0263.
- Klungland A, Robertson AB. Oxidized C5-methyl cytosine bases in DNA: 5-Hydroxymethylcytosine; 5-formylcytosine; and 5-carboxycytosine. *Free Radic Biol Med*. 2017;107:62–68. doi: 10.1016/j.freeradbiomed.2016.11.038.
- Luo J, Quan J, Tsai J, Hobensack CK, Sullivan C, Hector R, Reaven GM. Nongenetic mouse models of non-insulin-dependent diabetes mellitus. *Metabolism*. 1998;47:663–668.
- Kil IS, Lee JH, Shin AH, Park JW. Glycation-induced inactivation of NADP(+)-dependent isocitrate dehydrogenase: implications for diabetes and aging. *Free Radic Biol Med*. 2004;37:1765–1778. doi: 10.1016/j.freeradbiomed.2004.08.025.
- MacKenzie ED, Selak MA, Tennant DA, Payne LJ, Crosby S, Frederiksen CM, Watson DG, Gottlieb E. Cell-permeating alpha-ketoglutarate derivatives alleviate pseudohypoxia in succinate dehydrogenase-deficient cells. *Mol Cell Biol*. 2007;27:3282–3289.
- Illi B, Dello Russo C, Colussi C, et al. Nitric oxide modulates chromatin folding in human endothelial cells via protein phosphatase 2A activation and class II histone deacetylases nuclear shuttling. *Circ Res*. 2008;102:51–58. doi: 10.1161/CIRCRESAHA.107.157305.
- Fu Y, Dominissini D, Rechavi G, He C. Gene expression regulation mediated through reversible m⁶A RNA methylation. *Nat Rev Genet*. 2014;15:293–306. doi: 10.1038/nrg3724.
- Feng C, Liu Y, Wang G, Deng Z, Zhang Q, Wu W, Tong Y, Cheng C, Chen Z. Crystal structures of the human RNA demethylase Alkbh5 reveal basis for substrate recognition. *J Biol Chem*. 2014;289:11571–11583. doi: 10.1074/jbc.M113.546168.
- Lo MC, Aulabaugh A, Jin G, Cowling R, Bard J, Malamas M, Ellestad G. Evaluation of fluorescence-based thermal shift assays for hit identification in drug discovery. *Anal Biochem*. 2004;332:153–159. doi: 10.1016/j.ab.2004.04.031.
- Martinez Molina D, Jafari R, Ignatushchenko M, Seki T, Larsson EA, Dan C, Sreekumar L, Cao Y, Nordlund P. Monitoring drug target engagement in cells and tissues using the cellular thermal shift assay. *Science*. 2013;341:84–87. doi: 10.1126/science.1233606.
- Wu H, Zhang Y. Mechanisms and functions of Tet protein-mediated 5-methylcytosine oxidation. *Genes Dev*. 2011;25:2436–2452. doi: 10.1101/gad.179184.111.
- Barbati SA, Colussi C, Bacci L, Aiello A, Re A, Stigliano E, Isidori AM, Grassi C, Pontecorvi A, Farsetti A, Gaetano C, Nanni S. Transcription

- factor CREM mediates high glucose response in cardiomyocytes and in a male mouse model of prolonged hyperglycemia. *Endocrinology*. 2017;158:2391–2405. doi: 10.1210/en.2016-1960.
36. Kimes BW, Brandt BL. Properties of a clonal muscle cell line from rat heart. *Exp Cell Res*. 1976;98:367–381.
 37. Smith MJ, Taylor KW. Blood pyruvate and alpha-ketoglutarate in normal and diabetic subjects. *Br Med J*. 1956;2:1035–1038.
 38. Garella D, Atlante S, Borretto E, Cocco M, Giorgis M, Costale A, Stevanato L, Miglio G, Cencioni C, Fernández-de Gortari E, Medina-Franco JL, Spallotta F, Gaetano C, Bertinaria M. Design and synthesis of N-benzoyl amino acid derivatives as DNA methylation inhibitors. *Chem Biol Drug Des*. 2016;88:664–676. doi: 10.1111/cbdd.12794.
 39. Qi Y, Xu Z, Zhu Q, Thomas C, Kumar R, Feng H, Dostal DE, White MF, Baker KM, Guo S. Myocardial loss of IRS1 and IRS2 causes heart failure and is controlled by p38 α MAPK during insulin resistance. *Diabetes*. 2013;62:3887–3900. doi: 10.2337/db13-0095.
 40. Travers JG, Kamal FA, Robbins J, Yutzy KE, Blaxall BC. Cardiac fibrosis: the fibroblast awakens. *Circ Res*. 2016;118:1021–1040. doi: 10.1161/CIRCRESAHA.115.306565.
 41. Zeisberg EM, Kalluri R. Origins of cardiac fibroblasts. *Circ Res*. 2010;107:1304–1312. doi: 10.1161/CIRCRESAHA.110.231910.
 42. Intine RV, Sarra MP Jr. Metabolic memory and chronic diabetes complications: potential role for epigenetic mechanisms. *Curr Diab Rep*. 2012;12:551–559. doi: 10.1007/s11892-012-0302-7.
 43. Jayaraman S. Epigenetic mechanisms of metabolic memory in diabetes. *Circ Res*. 2012;110:1039–1041. doi: 10.1161/CIRCRESAHA.112.268375.
 44. Blomen VA, Boonstra J. Stable transmission of reversible modifications: maintenance of epigenetic information through the cell cycle. *Cell Mol Life Sci*. 2011;68:27–44. doi: 10.1007/s00018-010-0505-5.
 45. Salminen A, Kaarmiranta K, Hiltunen M, Kauppinen A. Krebs cycle dysfunction shapes epigenetic landscape of chromatin: novel insights into mitochondrial regulation of aging process. *Cell Signal*. 2014;26:1598–1603. doi: 10.1016/j.cellsig.2014.03.030.
 46. Mantri M, Zhang Z, McDonough MA, Schofield CJ. Autocatalysed oxidative modifications to 2-oxoglutarate dependent oxygenases. *FEBS J*. 2012;279:1563–1575. doi: 10.1111/j.1742-4658.2012.08496.x.
 47. Gillberg L, Ling C. The potential use of DNA methylation biomarkers to identify risk and progression of type 2 diabetes. *Front Endocrinol (Lausanne)*. 2015;6:43. doi: 10.3389/fendo.2015.00043.
 48. Yara S, Lavoie JC, Levy E. Oxidative stress and DNA methylation regulation in the metabolic syndrome. *Epigenomics*. 2015;7:283–300. doi: 10.2217/epi.14.84.
 49. Al-Mahdawi S, Virmouni SA, Pook MA. The emerging role of 5-hydroxymethylcytosine in neurodegenerative diseases. *Front Neurosci*. 2014;8:397. doi: 10.3389/fnins.2014.00397.
 50. Liyanage VR, Jarmasz JS, Murugesan N, Del Bigio MR, Rastegar M, Davie JR. DNA modifications: function and applications in normal and disease States. *Biology (Basel)*. 2014;3:670–723. doi: 10.3390/biology3040670.
 51. Greco CM, Kunderfranco P, Rubino M, Larcher V, Carullo P, Anselmo A, Kurz K, Carell T, Angius A, Latronico MV, Papait R, Condorelli G. DNA hydroxymethylation controls cardiomyocyte gene expression in development and hypertrophy. *Nat Commun*. 2016;7:12418. doi: 10.1038/ncomms12418.
 52. Joshi O, Wang SY, Kuznetsova T, Atlasi Y, Peng T, Fabre PJ, Habibi E, Shaik J, Saeed S, Handoko L, Richmond T, Spivakov M, Burgess D, Stunnenberg HG. Dynamic reorganization of extremely long-range promoter-promoter interactions between two states of pluripotency. *Cell Stem Cell*. 2015;17:748–757. doi: 10.1016/j.stem.2015.11.010.
 53. Kolodziejczyk AA, Kim JK, Tsang JC, Illic T, Henriksson J, Natarajan KN, Tuck AC, Gao X, Bühler M, Liu P, Marioni JC, Teichmann SA. Single cell RNA-sequencing of pluripotent states unlocks modular transcriptional variation. *Cell Stem Cell*. 2015;17:471–485. doi: 10.1016/j.stem.2015.09.011.
 54. Nakajima H, Kunitomo H. TET2 as an epigenetic master regulator for normal and malignant hematopoiesis. *Cancer Sci*. 2014;105:1093–1099. doi: 10.1111/cas.12484.
 55. Delatte B, Fuks F. TET proteins: on the frenetic hunt for new cytosine modifications. *Brief Funct Genomics*. 2013;12:191–204. doi: 10.1093/bfpg/elt010.
 56. Krokan HE, Bjørås M. Base excision repair. *Cold Spring Harb Perspect Biol*. 2013;5:a012583. doi: 10.1101/cshperspect.a012583.
 57. Wu H, Wu X, Zhang Y. Base-resolution profiling of active DNA demethylation using MAB-seq and caMAB-seq. *Nat Protoc*. 2016;11:1081–1100. doi: 10.1038/nprot.2016.069.
 58. Hardeland U, Steinacher R, Jiricny J, Schär P. Modification of the human thymine-DNA glycosylase by ubiquitin-like proteins facilitates enzymatic turnover. *EMBO J*. 2002;21:1456–1464. doi: 10.1093/emboj/21.6.1456.
 59. Fitzgerald ME, Drohat AC. Coordinating the initial steps of base excision repair. Apurinic/apyrimidinic endonuclease 1 actively stimulates thymine DNA glycosylase by disrupting the product complex. *J Biol Chem*. 2008;283:32680–32690. doi: 10.1074/jbc.M805504200.
 60. Bellacosa A, Drohat AC. Role of base excision repair in maintaining the genetic and epigenetic integrity of CpG sites. *DNA Repair (Amst)*. 2015;32:33–42. doi: 10.1016/j.dnarep.2015.04.011.
 61. Hubbard BP, Gomes AP, Dai H, et al. Evidence for a common mechanism of SIRT1 regulation by allosteric activators. *Science*. 2013;339:1216–1219. doi: 10.1126/science.1231097.
 62. Yu Q, Liu B, Ruan D, Niu C, Shen J, Ni M, Cong W, Lu X, Jin L. A novel targeted proteomics method for identification and relative quantitation of difference in nitration degree of OGDH between healthy and diabetic mouse. *Proteomics*. 2014;14:2417–2426. doi: 10.1002/pmic.201400274.
 63. Morgan PE, Sheahan PJ, Pattison DI, Davies MJ. Methylglyoxal-induced modification of arginine residues decreases the activity of NADPH-generating enzymes. *Free Radic Biol Med*. 2013;61:229–242. doi: 10.1016/j.freeradbiomed.2013.03.025.